Monocular vision for variable spray control system

Daozong Sun[1,2], Weikang Liu[1], Runmei Luo[1], Xurui Zhan[1], Zehong Chen[1], Tao Wei[1], Xinrui Wang[1], Xiuyun Xue[1,2,3], Zhen Li[1,2,3], Shuran Song[1,2,3*]

(1. *College of Electronic Engineering (College of Artificial Intelligence), South China Agricultural University, Guangzhou 510642, China*;
2. *Guangdong Engineering Research Center for Monitoring Agricultural Information, Guangzhou 510642, China*;
3. *National Citrus Industry Technology System Mechanization Research Laboratory, Guangzhou 510642, China*)

Abstract: The monocular vision-based system can obtain the leaf wall area characterizing the canopy parameter for online detection and real-time variable spraying, aiming to improve the accuracy of orchard spraying equipment and the utilization efficiency of pesticide. This study established a spraying system, in which canopy parameters were collected by monocular vision, and the spray volume decision coefficient was constructed by the leaf wall area and the L^* value in International Commission on Illumination Lab color space to control the duty cycle of each solenoid valve to achieve variable spraying. Four spray flow models were designed to determine the spray volume decision coefficient. The coefficients of determination of the spray volumes with the duty cycle range of 15% to 65% were all over 94 and the error of the leaf wall area values obtained using the improved super green algorithm (calculated as ExG = 2.1G–1.1R–1.1B) was only 0.5%. The test showed that there is a negative relationship between canopy denseness and L^*, and the value of L^* is smaller in the dense area compared with the sparse area; the actual flow generated by the system is similar to the theoretical flow when the duty cycle is 65%. The field validation tests showed that the variable spraying system could refine the droplet size and increase the droplet density to a certain extent with the same coverage rate, which had advantages over the continuous spraying. In terms of droplet deposition, $D_{V0.1}$ and $D_{V0.9}$ were reduced by 2 μm and 18 μm, respectively, and the increase of droplet density to 75 droplets/cm^2. At the same time, the improvement of droplet distribution uniformity and droplet penetration by 16% and 3%, respectively. Compared with continuous spraying, variable spraying can achieve 55.64% savings. The study demonstrates the feasibility of monocular vision in guiding spraying operations and provides a reference for the use of monocular vision in plant protection operations.

Keywords: monocular vision, leaf wall area, Lab color space, pulse width modulation, variable spraying
DOI: 10.25165/j.ijabe.20221506.7646

Citation: Sun D Z, Liu W K, Luo R M, Zhan X R, Chen Z H, Wei T, et al. Monocular vision for variable spray control system. Int J Agric & Biol Eng, 2022; 15(6): 206–215.

1 Introduction

Pesticides are playing an indispensable role in agricultural production, and at the same time, they play an extremely important role in protecting national food security[1]. The overuse of pesticides is not only wasteful, but also causes environmental pollution to varying degrees[2]. The issue of agricultural production becomes a hot topic of discussion in the worldwide, with the farm-to-table strategy aiming to de-crease the use of pesticides by 50% by 2030[3]. In 1989, Giles' team developed the idea of "application on-demand" for pesticide spraying[4]. Nevertheless, in the course of decades of development, the effective implementation of variable spraying has remained a vital issue that has been continuously explored by experts and scholars[5].

Although the continuous spraying can achieve high coverage during the spraying process, it ignores the canopy characteristics of different fruit trees and the differences between them, which usually results in over- or under-spraying of orchard fruit trees under continuous spraying conditions[6-8].

Variable spraying using canopy characteristics is a popular method of obtaining canopy characteristics that can increase the effective use of pesticides to varying degrees[9-11]. At present stage, the mainstream way to obtain canopy features is to use sensors, such as ultrasonic sensors, infrared sensors, distance sensors, LiDAR and vision sensors, etc[12-16]. Due to the continuous development of deep learning in recent years, the use of vision sensors has gradually increased compared to the previous ones, relying on their high accuracy and superior real-time characteristics to make effective progress in guiding variable spraying. Among them, Zhao et al.[17] accurately identified crops based on machine vision, and all the errors on target were less than or equal to 6.5 mm, achieving accurate spraying on target; Yan et al.[18] obtained the vineyard canopy volume based on binocular vision cameras, and the success rate of identifying canopy reached 93.3%, and the variable spraying system developed could save

Received date: 2022-04-28 **Accepted date:** 2022-09-16
Biographies: Daozong Sun, PhD, Associate Professor, research interest: agricultural electrification and automation, Email: sundaozong@scau.edu.cn; **Weikang Liu,** MS, research interest: on-farm precision spraying, Email: liuweikang@stu.scau.edu.cn; **Runmei Luo,** MS, research interest: the use of deep learning in agriculture, Email: runmei@stu.scau.edu.cn; **Xurui Zhan,** MS, research interest: on-farm precision spraying, Email: langzizhan@stu.scau.edu.cn; **Zehong Chen,** MS, research interest: on-farm precision spraying, Email: 1322855404@qq.com; **Tao Wei,** UG, research interest: on-farm precision spraying, Email: 1317223009@qq.com; **Xinrui Wang,** UG, research interest: on-farm precision spraying, Email: 1374759336@qq.com; **Xiuyun Xue,** PhD, Associate Professor, research interest: spraying technology, Email: xuexiuyun@scau.edu.cn; **Zhen Li,** PhD, Professor, research interest: agricultural information technology, Email: lizhen@scau.edu.cn.

***Corresponding author: Shuran Song,** PhD, Professor, research interest: agricultural electrification and automation, spraying technology. College of Electronic Engineering (College of Artificial Intelligence), South China Agricultural University, Guangzhou 510642, China. Tel: +86-13668966908, Email: songshuran@scau.edu.cn.

55.27% of medicine; Miella et al.[19] used machine vision technology to achieve accurate calculation of canopy volume in a vineyard and to enable quantitative fruit production counting. However, canopy volume requires the calculation of three-dimensional data, resulting in a large computational effort. Some scholars have guided spraying based on leaf wall area as a way to achieve precision spraying. In particular, the LWA has been identified as a good compromise between accuracy and simplicity to establish a linear relationship between canopy geometry and the recommended amount of PPP[20]. Xue et al.[21] constructed a precision application model based on leaf wall area, with a 68.34% saving rate.

The CIELab color space system is the most complete color model customarily used to describe all colors visible to the human eye[22,23]. It has achieved good results in the evaluation of color shades. Wang et al.[24] showed that the brightness, chroma and saturation of wine were significantly correlated with CIELab.

Monocular vision is widely used in autonomous mobile spraying robots in orchards due to its simple structure, mature algorithms and low computational effort[25]. Monocular vision technology is less constrained by external environmental factors such as air temperature, humidity and wind speed. It is more stable than the use of canopy parameters such as ultrasonic sensors, infrared sensors and so on. Besides, using monocular vision techniques to obtain 2D data such as canopy area instead of 3D point cloud data processing. It can effectively avoid problems such as excessive data volume and inefficient processing. In spite of this, monocular vision technology is still not widely used in plant protection operations and the research was conducted to explore the feasibility of monocular vision technology in plant protection operations. For this reason, based on the above-mentioned features of monocular vision, the study uses monocular vision to obtain canopy parameters, which are used to model the application rate according to the LWA (Leaf Wall Area) and L* value (The Color Lightness) of the canopy image, and to correlate the effect of variable sprays through field trials.

2 Materials and method

2.1 Experimental materials

The principal components of the variable spray system in the study were shown in Figure 1. The overall spraying system can be divided into a detection unit and a spraying unit. The detection unit uses a LifeCam HD-3000 monocular camera (Microsoft, Redmond, Washington, USA) was used to capture HD quality video at 30 fps and TrueColor technology automatically provided bright and rich video in almost all lighting conditions, while the data collected from the experiments can be saved to a laptop. The spraying unit is mainly controlled by an STM32F103 (Minimum system board, STMicroelectronics N.V., Geneva, Switzerland). The spray unit was fitted with a standard solid conical nozzle JJXP-010-PVDF (H. Ikeuchi & Co., Ltd., Nishi-ku, Osaka, Japan) and a solenoid valve with an operating pressure of up to 1 MPa (DELIXI Group Co., Ltd., Zhejiang, China). Spraying unit was installed at a height of 1.2 m above the ground, with a group of spraying devices installed at 50 cm intervals, making a total of four groups of spraying devices, which showed in Figure 2. The liquid was pumped out of the tank by a diaphragm pump, through a pipe into each solenoid valve, and delivered by the solenoid valve to each nozzle. Considering that the rated pressure of the nozzle was 0.2 MPa, the spraying pressure in the experiment was designed at 0.3 MPa for better spraying results.

Water-sensitive papers (76 mm×26 mm, Syngenta Crop Protection AG, Basel, Switzerland) were used to collect data such as droplet deposition. The water-sensitive papers were then scanned and images were produced at a resolution of 600 dpi using an HP Color Laser Jet Pro MPF M479dw printer with integrated scanner (HP, PaloAlto, California, USA). A specially programmed image processing macro in DespiteScan (National Institutes of Health, Bethesda, MD, USA) was used to determine the spray coverage parameters.

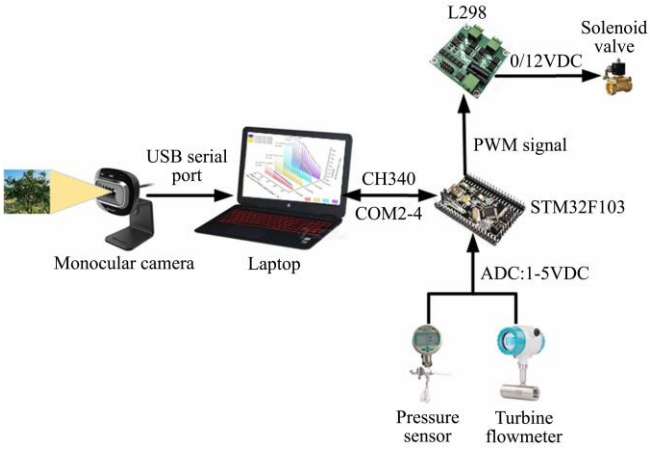

Figure 1 Composition of variable spray control system

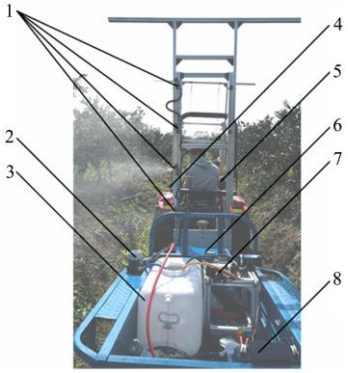

1. Nozzles 2. Turbine flowmeter 3. Pesticide tank 4. Monocular camera 5. Laptop 6. Pressure sensor 7. Diaphragm pump 8. Battery

Figure 2 Overall structure of variable sprayer

2. 2 Experimental design and methodology

2.2.1 Calculation of LWA

In order to provide an accurate reference value for LWA calculation based on monocular vision, the study was conducted based on the Excess Green Index (ExG) proposed by Woebbecke[26] for LWA calculation.

In order to obtain a true LWA of the simulated tree, the simulated tree was placed in an open area to avoid the presence of green objects around it, and a red square reference with a side length of 10 cm was prevented at the base of the trunk as a dimensional reference, and a monocular camera was used to capture an image of the fruit tree at 1.5 m from the front, as shown in Figure 3. Using the ExG to obtain the area of the square reference in the image acquired by the monocular camera at this time. The ExG was as follows:

$$ExG = 2G - R - B \quad (1)$$

where, ExG is the Excess Green Index; G, R, B are the green, red and blue components of the acquired image.

The area of the square reference in the image is compared with the actual reference to obtain its scale factor k, from which the area of the tree canopy can be calculated from the area of the reference in

the image; after processing by the super green algorithm, the total number of white pixel points N_{sum} in the image can be obtained directly. The calculation of leaf wall area LWA was as follows:

$$LWA = \left(\frac{\sqrt{N_{sum}}}{k} \times 50 \right)^2 \quad (2)$$

where, LWA is the leaf wall area, cm^2; N_{sum} is the total number of white pixel points in the image; and k is the scale factor.

To make the obtained LWA values closer to the true values, an adjustment was made to ExG. The improved ExG was as follows:

$$ExG = 2.1G - 1.1R - 1.1B \quad (3)$$

The procedures are the same as above for obtaining LWA by the improved ExG.

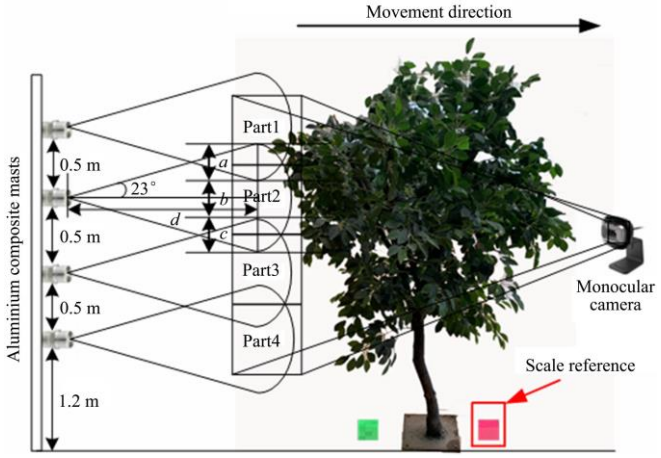

Note: 1. The part 1-part 4 represent the area of the image captured by the monocular vision and corresponds to the main area sprayed by the four nozzles. The areas move in the same direction as the machine travels. 2. According to pre-experiments, the nozzle atomisation angle is 46°±2°. And Comparing target distances of 1 m, 1.25 m and 1.5 m, the design of the sprayer is more effective when the target distance is set at 1.5 m. And the atomisation range is approximately 1.2 m according to the Pythagorean theorem. According to the nozzle technical manual, there will be no spray volume in area b and approximately half the spray volume is lost in areas a and c. Therefore the two nozzles are used for overlapping to make up for the spray volume, i.e. as shown in the diagram. 3. In the diagram *a* and *c* represent spray areas where spray is lost and *b* represents areas where no spray is lost, *a*, *b* and *c* are all 0.4 m. And the *d* represents the target distance and is set at 1.5 m.

Figure 3 Detection segmentation of canopy parameter

Figure 4a shows the original binary image of the simulated tree, which has the sparse canopy on the inside. According to the design parameters of the simulated tree used in the experiment, the real projected area of the simulated tree canopy is 17671.4 cm^2, and the area corresponding to the white pixel point of this binary image is 17539.6 cm^2 calculated directly, resulting in a small calculated value. The improved binary image is shown in Figure 4b, which corresponds to an LWA calculation value of 17587.5 cm^2, and its LWA value is close to the true value, with an error reduction of 0.5%, so the study uses the improved ExG as the LWA calculation algorithm.

2.2.2 Color space design verification methods

As it is difficult to adjust the spray volume to the canopy density of the monocular camera images, the color brightness L^* of the International Commission on Illumination Lab (CIELab) color space was added as a reference to the canopy density. In order to investigate the relationship between canopy density and L^*, images of fruit trees were taken with a monocular camera at 1.5 m from the front and several images were taken with different degrees of canopy sparsity. Since RGB cannot be directly converted to CIELab, it was first converted to *XYZ*, and the formula was as follows:

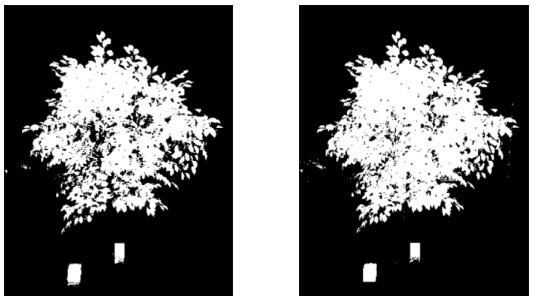

a. Original binary image b. Improved binary image

Figure 4 Canopy binary image of simulation tree

$$\begin{bmatrix} X \\ Y \\ Z \end{bmatrix} = \begin{bmatrix} 0.412453 & 0.357580 & 0.180423 \\ 0.212671 & 0.715160 & 0.072169 \\ 0.019334 & 0.119193 & 0.950227 \end{bmatrix} \begin{bmatrix} R \\ G \\ B \end{bmatrix} \quad (4)$$

where, X, Y, Z represent the proportion of red primary color, the proportion of green primary color and the proportion of blue primary color, respectively.

Obtain *XYZ* values according to Equation (4) and convert them to CIELab values, the calculation was as follows:

$$\begin{cases} L^* = 116 f(Y/Yn) - 16 \\ a^* = 500[f(X/X_n) - f(Y/Y_n)] \\ b^* = 200[f(Y/Y_n) - f(Z/Z_n)] \end{cases} \quad (5)$$

$$f(t) = \begin{cases} t^{1/3} & \text{if } t > \left(\frac{6}{29}\right)^3 \\ \frac{1}{3}\left(\frac{6}{29}\right)^2 t + \frac{4}{29} & \text{otherwise} \end{cases} \quad (6)$$

where, L^*, a^* and b^* represent the luminance value of the pixel, the range from red to green and the range from yellow to blue respectively, and X_n, Y_n and Z_n are the white point reference values for the D65 light source, where X_n is 0.950456, Y_n is 1 and Z_n is 1.088754.

2.2.3 Model construction method for application rate calculation

The decision to apply pesticides is based on the LWA and L^* values of the fruit tree. The decision coefficient S of the LWA-based application rate calculation model in the study is denoted as S_{LWA}. Based on the actual situation, it is difficult to reasonably determine the application rate using single leaf wall area. Therefore the study relies on the literature[22], and the decision coefficient S_{LWA} will be determined by weighting two characteristic parameters, namely LWA and the L^* component of the CIELab color space in which the RGB of the leaf wall image is processed. Finally, considering the leaf wall weighted allocation of area S_1 was set to 60%, and the model was calculated as follows:

$$S_{LWA} = 0.6S_1 + 0.4S_2 \quad (7)$$

where, S_1 represents the area of the leaf wall in the area of monocular vision acquisition and S_1 is equal to LWA, cm^2; S_2 represents the L^* component of the CIELab color space where the canopy image RGB is located.

After obtaining the decisive factor S_{LWA}, the flow rate of required spray in real time was obtained by means of the application volume calculation model, the calculation used was as follows:

$$Q_{flow} = \rho v(a + b\, S_{LWA}) \quad (8)$$

where, Q_{flow} is the required spray flow rate, a and b are determined by the nozzle flow model; v is the machine travel speed, m/s; ρ is the spray volume adjustment factor, based on the actual control needs of each orchard, and the application factor is determined according to the recommended dosage by the pharmaceutical manufacturer and field trials, and ρ is defined as 1 based on reference to the research of some scholars[27-29].

There are certain differences in the canopy of fruit trees in both the vertical and horizontal directions, and the nozzle radiation range is relatively limited. In order to be able to achieve accurate calculation of leaf wall area and apply medicine on demand, according to the actual situation of citrus trees in the orchard, as shown in Figure 3, the canopy is evenly divided into four spray areas in the vertical direction. In the process of calculating the partitioned LWA, the partition size of visual calculation area in horizontal and vertical direction are consistent while splitting the area in the horizontal direction.

Based on the application volume calculation model designed above, the study also needed to design the corresponding multi-nozzle flow model. In order to avoid a large impact of PWM on the spray quality, PWM-based control of the solenoid valve opening and closing was used in the study[5]. The operating frequency of the solenoid valve was set to 10 Hz to ensure the spray uniformity, the variation range of spray flow and the solenoid valve response. To avoid the poor response of the solenoid valve due to the high spray pressure when the duty cycle is too small[30], the spray pressure was set to 0.3 MPa.

The study conducted calibration tests of spray flow under the above conditions, but a multi-nozzle variable spray system is no longer a simple superposition of the spray characteristics of single nozzle[31]. Therefore, in the initial stage of the calibration test of multi-nozzle spray flow model, the spray pressure (0.3 MPa), the PWM frequency of the solenoid valve (10 Hz) and the spray time (10 s) were controlled and calibration tests of multi-nozzle flow were carried out by turning on different numbers of nozzles (1, 2, 3 and 4) with different PWM duty cycles (10% to 100% with an increment of 5%). A multi-nozzle variable spray model was built.

2.2.4 System performance verification tests

A prototype system was built to verify the performance of the system before field trials to test whether the actual spray volume was linear to the ideal spray volume. The specific design of the trial was to use pure water instead of pesticide, ignore differences between spray nozzles and select an arbitrary spray nozzle to test, while nozzle 2 was tested in the validation trial. Inputting the LWA for 1000 cm^2 and the L^* for 0 as the simulation input of nozzles 1, 3 and 4, which is the maximum flow rate. The leaf wall area of nozzle 2 was set as 500, 400, 300, 200, 175, 150, 125, 125, 125, 125 and 100 cm^2, respectively, while L^* were correspondingly used the value of 50, 60, 70, 80, 85, 85 85, 50, 60 and 70, respectively. The simulated test included 8 groups, the flow of nozzle 2 was calibrated alone before the test began each time. Fixing the drying kettle in front of nozzle 2, the system prototype was started to test at a speed of 1 m/s while each simulated test continued for 10 s. The drying kettle was removed while the test was ended. An electronic balance with the accuracy of ±0.001 g for weighing was used to convert the spray flow rate values of nozzle 2 at multiple simulated input values.

2.2.5 Field trials

To test the effectiveness of field spraying, 12 times field trials were conducted at the Orange Orchard Pingtan site in Pingtan Town, Huidong County, Huizhou City, Guangdong Province, China. Field trials were conducted from 7 January 2022 to 9 January 2022. The ambient temperature, ambient humidity and average wind speed during the trial are 25℃-30℃, 45%-52%, and less than 0.7 m/s, respectively. Test subjects were citrus trees with a row spacing of 1.2 m.

Due to the symmetrical characteristics of the monocular vision camera detection angle, variable spray characteristics tests were conducted on only one side of the tree canopy in this paper.

In the orchard precision variable spraying process, the variable spraying decision system response time t_0 is 212.5 ms and is calculated as shown in Equation (9):

$$t_0 = t_{01} + t_{02} + t_{03} \quad (9)$$

where, t_{01} represents the monocular vision camera response time, 40 ms; t_{02} represents the MCU response time, 12.5 ms; and t_{03} represents the variable spray system execution time, 160 ms.

At the same time, to avoid mist droplets drifting and wetting the lens to affect the image quality of the camera, the camera was placed 2 m away from the spraying device and a plastic box was installed around the camera to ensure that the camera would not be wetted by the mist droplets.

The spray nozzles were placed directly in front of the canopy and divided into four layers from top to bottom. Each layer was evenly distributed with three sheets of sampling water-sensitive papers, which numbered 1 to 12 from left to right and then from top to bottom, respectively. The distribution of sampling water-sensitive papers is shown in Figure 5. In order to demonstrate the good representativeness of the test results, three trees were arbitrarily selected as sampling points during the test.

a. Layout schematic diagram b. Filed test

Figure 5 Layout of water sensitive paper of liquid adhesive test

After completing the work on the water-sensitive paper arrangement, pure water was used instead of the liquid. The test was set up with a spray pressure of 0.3 MPa, the targeted distance was set to 1.5 m.

Pre-test to obtain the optimum spraying speed of 1m/s and a maximum operating speed of 1.5m/s. So the speed of the sprayer was set to 1 m/s for the field spray test with a travel distance of 30 m. Firstly, the continuous spraying mode was switched on and the machine performed three continuous spraying operations at a speed of 1 m/s. Afterward, the variable spraying mode was switched on and the machine performed three variable spraying operations at a same speed as the continuous spraying mode. After each testing, the water-sensitive papers were removed in order with disposable gloves and stored in a sealed dry box to protect them from moisture. Then, the water-sensitive papers were scanned in the laboratory by using a scanner in accordance with DespiteScan software. The measurement parameters for the experimental evaluation of droplet size are $D_{V0.1}$, $D_{V0.5}$ and $D_{V0.9}$, where $D_{V0.5}$, also known as the median droplet volume diameter (VMD), is one of the most commonly used indicators of droplet size. D_{Va} (a=0.1, 0.5, 0.9) indicates the droplet size when all droplets in a spray are added up in descending order of volume and the total value is equal to (a×100%) of the total droplet volume.

R_S was utilized to indicate the distribution of droplets on the fruit tree, which reflects the uniformity of the droplet distribution. The smaller the R_S, the more uniform the droplet distribution.

When R_S is equal to 1, it means that the droplet size is symmetrically distributed, and the droplet distribution span was calculated as follows:

$$R_S = \frac{D_{V0.9} - D_{V0.1}}{VMD} \tag{10}$$

To evaluate the effect of the fog droplet penetration in different canopy areas, $D_{V0.5}$ was viewed as the base parameter and the coefficient of variation CV was used to measure the fog droplet penetration between sampling points within the canopy area. A smaller coefficient of variation represents a stronger performance of the fog droplet penetration. The coefficient of variation was calculated as follows:

$$CV = \frac{S}{\bar{X}} \times 100\% \tag{11}$$

$$S = \sqrt{\sum_{i=1}^{n} (X_i - \bar{X})^2 / (n-1)} \tag{12}$$

where, S is the standard deviation of the VMD for different cases, μm; X_i is the median straight VMD of the droplet volume for different cases, μm; $\bar{X}$ is the mean value of the median droplet volume diameter VMD for different cases, μm; and n is the number of groupings for different cases.

3 Results and discussion

3.1 Results and analysis of the association between CIELab color space and canopy densities

The canopy images obtained by the monocular vision were converted using CIELab color space, and the results are listed in Table 1. The L^* values of the canopy images obtained are small, denoting the small luminance, because the leaves in the dense areas are not overshadowed. The L^* values of the canopy images obtained are large, denoting the high luminance, because the leaves in the sparse areas are not overshadowed. For this reason, when comparing several sets of test data, it is clear from the selected areas in Figure 6 and the data in Table 1 that the L^* value in the sparse areas is significantly greater than that in the dense areas, which have more leaves, resulting in a smaller overall L^*. The difference in densities between areas 1 and 3 and areas 4 and 6 is small, and according to Table 1, the L^* values are similar, whereas areas 2 and 5 are both dense areas with small L^* values. But according to Figure 6, area 2 is sparser than area 5, and the L^* value of area 2 is larger than that of area 5. The L^* value is limited by the densities in the area. Then, the smaller L^* demonstrates the denser canopy. For this reason, the L^* component S_2 of the CIELab color space in which the canopy RGB is located within the sub-area of the spray decision factor S_{LWA} is defined as follows:

$$S_2 = (100 - L^*) \times 100\% \tag{13}$$

Table 1 Orthogonal experiment data table

Area of the tree	B	G	R	L^*	a^*	b^*
1	204.119	208.391	210.304	92.469	–7.911	–4.203
2	95.326	113.234	100.108	71.422	–12.088	1.458
3	200.784	205.493	204.823	91.862	–8.331	4.208
4	170.867	176.857	177.942	86.641	–7.812	–3.351
5	29.837	44.135	34.164	47.068	–13.302	6.291
6	170.591	178.788	176.137	86.830	–8.716	–3.004
7	237.775	239.050	243.630	97.669	–7.652	–5.097
8	178.962	183.129	187.112	87.983	–7.215	3.768
9	244.666	245.379	250.107	98.671	–7.669	–5.272

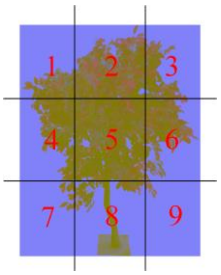

Figure 6 Canopy subdivision and CEILab processing

3.2 Results and analysis of model construction for application rate calculation

The test process found that in the case of multiple nozzles, the duty cycle of more than 65%, the flow rate changes less than 2% and is basically constant, while the flow rate is smaller in the duty cycle of less than 15%. These situations are not effective to form droplets, so the duty cycle was set from 15% to 65%. The specific spray flow and linear fit results are shown in Figure 7, the model for the linear fit, the coefficient of determination of the model R^2 is greater than or equal to 0.94, indicating that while the duty cycle changes in the range of 15% to 65%, the nozzle flow and duty cycle has a strong linear relationship. Comprehensive consideration, the choice of duty cycle of 15% to 65% range, based on the number of nozzles, the relationship between flow rate and duty cycle is shown as follows:

$$\begin{cases} Q_1 = \dfrac{0.00751\alpha + 0.48497}{1} \\ Q_2 = \dfrac{0.01533\alpha + 0.71617}{2} \\ Q_3 = \dfrac{0.03991\alpha + 0.55574}{3} \\ Q_4 = \dfrac{0.04441\alpha + 0.80091}{4} \end{cases}, \quad 15 \le \alpha \le 65 \tag{14}$$

where, Q_1-Q_4 are all spray nozzle spray flow rates at 0.3 MPa spray pressure, L/min; α is the pulse width modulation (PWM) control signal duty cycle, %.

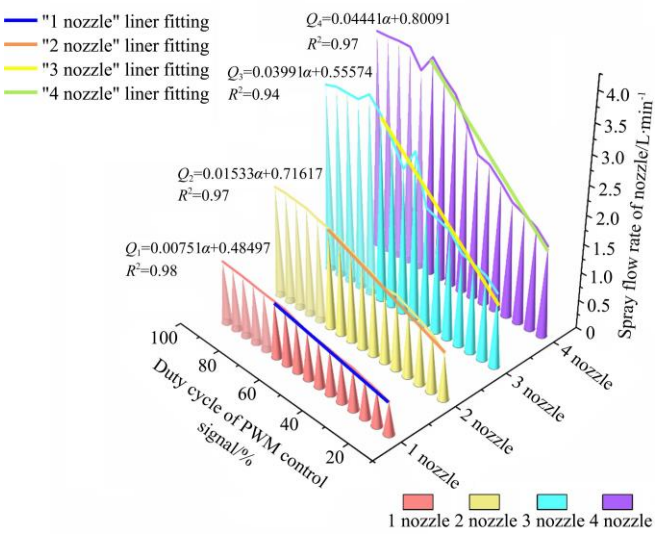

Note: In the legend, n nozzles (n=1, 2, 3 and 4) represent the number of open nozzles. Figure 6 shows the spray flow rates corresponding to different duty cycles when different numbers are switched on. The solid cone represents the data for the effective range and the hollow cone represents the data for the ineffective range. The valid data are fitted linearly in the graph.

Figure 7 Liner fitting results of duty cycle of PWM control signal and spray flow rate of nozzle

To facilitate the application volume decision in the program, α is calculated from the nozzle flow model, i.e., its corresponding percentage of control solenoid PWM duty cycle, noted as D.

Equation (14) is collated as:

$$\begin{cases} D=0,\ \alpha<15 \\ D=\alpha=\dfrac{Q_i-b}{a},\ 15\le\alpha\le65 \\ D=100,\ \alpha>65 \end{cases} \quad (15)$$

The maximum effective duty cycle of 65% and the minimum effective duty cycle of 15% were substituted into Equation (14), respectively, to obtain a different number of nozzles open when single nozzle corresponds to the maximum and minimum flow values, the number of different nozzles open when single nozzle corresponds to the maximum and minimum flow values are listed in Table 2.

Table 2 Flow extremes of a single nozzle for different numbers of open nozzles

Flow rate for single nozzle	Number of nozzles			
	1	2	3	4
Maximum/L·min^{-1}	0.97312	0.85631	1.04996	0.92189
Minimum/L·min^{-1}	0.59762	0.47306	0.3848	0.36677

To calibrate the coefficients a and b of Equation (8), and to ensure that the number of different nozzles open state, the solenoid valve PWM duty cycle using Equation (15) are between 15%-65%, take 0.59762 as the solenoid valve PWM duty cycle of 15% of the flow value, the corresponding decision coefficient S for non-zero minimal value, take 0.92189 as the solenoid valve PWM duty cycle of 65% of the flow value, the corresponding The decision factor S_{LWA} is 1, at this time the system's flow regulation range is 0.59762-0.92189, which can be organized into the specific expression of Equation (8) as:

$$Q_{flow}=\rho_v(0.59762+0.32427\ S_{LWA}) \quad (16)$$

Equations (8), (15) and (16) are collapsed to obtain the application rate calculation model, which is given by

$$\begin{cases} D=0,\ \alpha<15 \\ D=\dfrac{\rho_v(0.59762+0.32427\cdot S_{LWA})-0.32427}{0.59762},\ 15\le\alpha\le65 \\ D=100,\ \alpha>65 \end{cases} \quad (17)$$

3.3 Validation test results and analysis

During the application consistency verification of the prototype, the LWA and L^* values were simulated for a variety of scenarios and the results are listed in Table 3. The actual flow rate of the system was found to be consistent with the ideal flow rate. The actual spray flow rate was the closest value to the ideal flow rate with the duty cycle greater than 65%. The actual flow rate was found to be greater than the ideal flow rate when the input simulated LWA and L^* values were of smaller with the duty cycle less than 65%, but the fluctuation was small with the averaging value of 0.013 L. During the testing process, there may be a certain error in the test process, the results basically match the ideal flow rate value within the error tolerance. Additionally, the actual flow rate is greater than the ideal flow rate by using smaller LWA and larger L^* values in relatively sparse areas of the canopy. Although it may cause an overdosing in some areas, it can effectively prevent the occurrence of sparse areas such as missed spraying.

3.4 Results and analysis of the filed trial

Water sensitive paper was analyzed using DespiteScan software after several trials with both constant and variable spray, and the spray effect of two spray methods are shown in Figure 8.

With the additional installment of the variable spray system, the test specimen performed better overall in terms of droplet deposition than before the modification, although there was a slight reduction in droplet coverage. The atomization parameters for the 2 spraying methods are listed in Table 4.

Table 3 Simulated system flow test results for the leaf wall area and L^* values

Simulated LWA/cm^2	Simulated L^* value	Duty cycle/%	Flow value/L	
			Theoretical flow value/L	Actual flow value/L
500	50	73	0.154	0.156
400	60	67	0.154	0.150
300	70	62	0.116	0.136
200	80	57	0.110	0.124
175	85	55	0.109	0.122
150	85	54	0.108	0.119
125	85	53	0.107	0.111
125	50	61	0.115	0.130
125	60	58	0.112	0.126
100	70	56	0.109	0.122

a. Continuous spray b. Variable spray

Figure 8 Spray effect under two spraying modes

Table 4 Flow extremes of a single nozzle for different numbers of open nozzles

Spraying modes	$D_{V0.1}$ /μm	$D_{V0.9}$ /μm	VMD /μm	Droplet density /cm^{-2}	Coverage /%
Continuous spray	107	288	162	48	33.132
Variable spray	105	270**	157	75**	31.052

Note: Significant differences between the two groups of data were analysed using *t*-tests. * indicates a significantly difference ($0.01<p<0.05$). ** indicates a highly significant difference ($p<0.01$). The same as below.

3.4.1 Analysis of droplet distribution

As can be seen from Table 4, the droplet size is larger with continuous spraying than with variable spraying. 2 μm is reduced by $D_{V0.1}$, while 18 μm is reduced by $D_{V0.9}$, and a highly significant difference is found. The range of droplet size changes is consistent with the results of Thomas et al.[32], which demonstrates that the variable spraying can refine the droplet size due to the PWM response process. The output signal of PWM will drive the solenoid valve to open and close rapidly, and the flow rate of the liquid in the pipeline will change instantaneously as a result, leading to large fluctuations in pressure at the nozzle, resulting in water hammer[33]. At the same time, the difference between $D_{V0.1}$ and $D_{V0.9}$ becomes smaller, denoting that the difference in droplet size becomes smaller under variable spraying. According to relevant research[34], there is a tendency to behave alike within similar size droplets, which tend to carry out similar trajectories for drifting movement. If there is a large difference in droplet size in the spraying process, it will lead to a certain degree of droplet separation from the target, resulting in Severe droplet drift and poor droplet deposition distribution.

Therefore, the droplet distribution uniformity was further analyzed. Based on the droplet distribution span R_S as a measure of the droplet deposition uniformity, and the results are listed in Table 5.

Table 5 Flow extremes of single nozzle for different numbers of open nozzles

Spraying modes	R_S
Continuous spray	1.12
Variable spray	1.05**

According to Table 5, after variable spraying, the droplet distribution span is relatively concentrated and the results are better than those of the continuous spraying method. The span of distribution under the variable spraying method was 1.05, a 16% decrease in droplet span compared to the continuous spraying method, with a narrower droplet spectrum and a more concentrated droplet particle size distribution obtained. Compared to the droplet distribution span of 1.41 obtained by Maghsoudi et al.[35], the variable spraying system studied in the paper resulted in a more uniform droplet distribution.

In summary, the variable spraying method has certain guiding significance for pesticide spraying. Obtaining a suitable PWM duty cycle can refine the droplet size, effectively reduce the droplet size distribution span and droplet drift, obtain a relatively uniform droplet size and improve the application quality.

3.4.2 Analysis of droplet penetration

During the test, it was found that the droplets were more penetrating during the variable spraying process due to the water hammer phenomenon. Therefore, the droplet penetration was further investigated and the droplet penetration was obtained in two different ways, as shown in Figure 9.

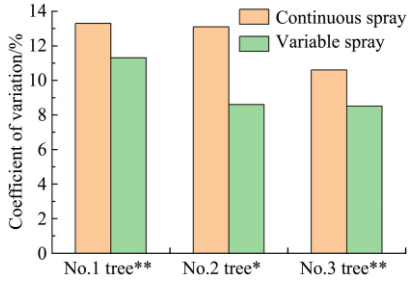

Note: 1. The first marked fruit tree is on the left; the second marked fruit tree is in the middle; the third marked fruit tree is on the right.

2. Significant differences between the two groups of data were analysed using *t*-tests. * indicates a significantly difference ($0.01<p<0.05$). ** indicates a highly significant difference ($p<0.01$).

Figure 9 Droplet penetration

The smaller coefficient of variation represents the more penetrating of the droplets. The coefficient of variation for droplet penetration under continuous spraying is in the range of 10.6% to 13.3%, while the coefficient of variation for droplet penetration under variable spraying is in the range of 8.5% to 11.3%, which is significantly lower than that under continuous spraying.

After dividing the canopy into three layers, the droplet penetration was found to be generally weak in the middle and strong on both sides, as shown in Figure 10. The main reason for this may be that the middle canopy is larger in LWA and much denser than the two sides of the canopy, which affects the droplet penetration performance compared to the two sides of the canopy. Nevertheless, the droplet penetration after outputting a suitable PWM duty cycle is still better than that of the continuous spraying method.

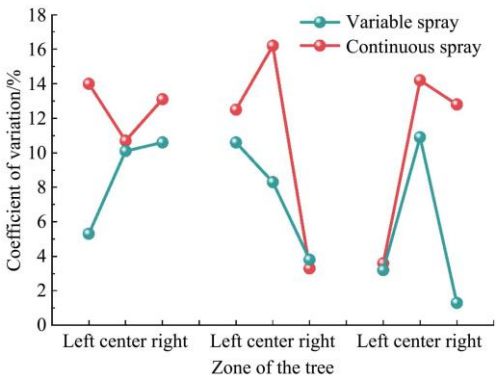

Note: The first marked fruit tree is on the left; the second marked fruit tree in the middle; the third marked fruit tree on the right.

Figure 10 Droplet penetration in different areas of the tested trees

3.4.3 Analysis of droplet coverage

Figures 11 and 12 show the results of spray coverage for the continuous and variable spraying methods. According to the results, there was no significant difference in coverage in most areas between the 2 spraying methods. Furthermore, the spray coverage was more uniform with the variable spraying method. As can be seen from Table 4, there was no significant variability in spray coverage with the variable spraying method and there was sufficient coverage for orchard spraying. This indicates that good spray coverage can still be achieved even with less application. Similar findings have been made by other authors, such as the spray volume study on olive trees by Pérez-Ruiz et al.[36] and the variable spray study on grapevines by Yan et al.[18]. However, the variable spraying system developed in the paper had a spray coverage loss of only 2.08%, much smaller than that of the continuous spraying.

3.4.4 Analysis of droplet coverage

The droplet density of the variable spraying method is significantly higher than that of the continuous spraying method, the average coverage density is 75 droplets/ cm^2, as shown in Table 4. Test results are shown in Figures 13 and 14. According to the performance of water-sensitive paper at the actual test site, after variable spraying, combined with the analysis in section 3.4.1, similar size droplets have a tendency, that is, the variable spraying method under the droplet similarity is greater, resulting in droplets collisions and secondary collisions in the air. Therefore, more fine droplets with uniform distribution were produced. In contrast to the continuous spraying method, although the droplet coverage is good, the droplets of the variable spraying are mostly small droplets that reach the canopy and then recoalesce into large droplets, resulting in larger droplet sizes. The continuous spraying method is less penetrating and the droplets bind to the canopy surface, forming large droplets. The variable spraying method avoids such problems, as it has a stronger droplet penetration in dense canopy areas, which prevents droplets from forming secondary binding on the canopy surface and large droplets, while it avoids wasting the solution in sparse canopy areas. The average droplet density on different canopies of the orchard was slightly increased by 15 droplets/cm^2 compared to the variable sprayer developed by Li et al.[28], and by 40 droplets/cm^2 compared to the variable sprayer developed by Fan et al.[37]

In conclusion, the variable spraying equipment developed in the study has advantages in improving the droplet size and the spatial distribution that continuous spraying does not have. It has the better droplet coverage density than the variable spraying systems developed by some scholars.

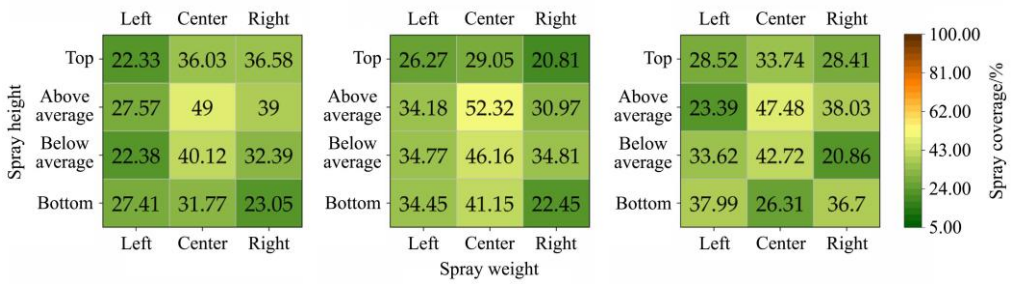

Note: The first marked fruit tree is on the left; the second marked fruit tree is in the middle; the third marked fruit tree is on the right. The same as below.

Figure 11 Continuous spray coverage

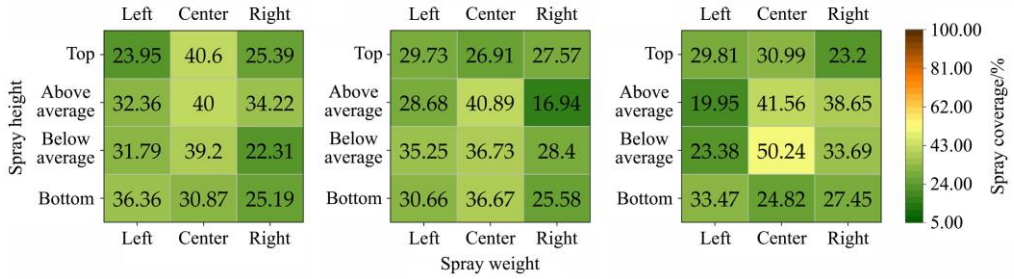

Figure 12 Variable spray coverage

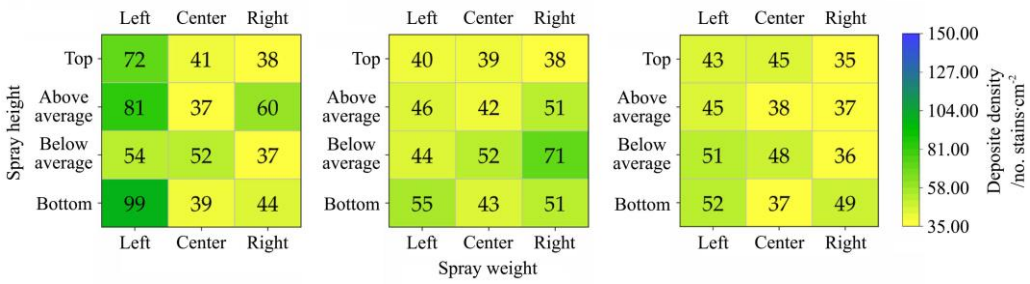

Figure 13 Continuous spray droplet density

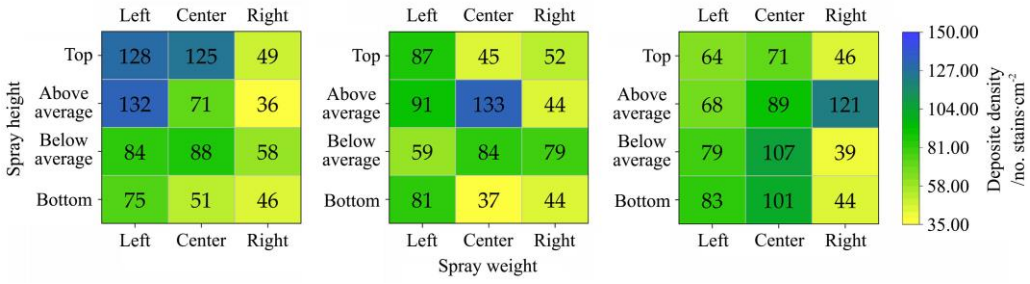

Figure 14 Variable spray droplet density

3.4.5 Analysis of drug saving rates

As shown in Table 6, the average spray flow rate during continuous spraying was 4.838 L/min, regardless of leaf wall size and canopy densities. The application rates of two different spraying patterns within 30 m of the machine were obtained from the test. Compared with the continuous spraying, the variable spraying pattern saved about 55.64% of pesticide dosage and lost only 2.08% of spray coverage. The variable spraying method proposed by Yan et al.[18] saved about 55.27% of the pesticide dosage in a continuous intensive orchard. The savings and coverage loss rates in this paper were broadly consistent with them. The results of the variable spraying method proposed by Xue et al.[21] on monocot type simulation trees showed that compared with continuous spraying and quantitative spraying on the target, the savings of variable spraying were 68.34% and 32.77%, respectively. The main reason for the higher savings of the variable spray system than its counter-target quantitative spray, but lower than its variable spray, may be that the variable spray system in the study is slightly lower than its monoculture sparse orchard savings due to the lower clearance between the fruit trees in the trial site compared to the monoculture simulated trees due to the more vigorous growth of citrus trees.

Table 6 Flow extremes of single nozzle for different numbers of open nozzles

Spraying modes	Dosage of pesticide/L	Average spray flow/L·min^{-1}
Continuous spray	2.419	4.838
Variable spray	1.073**	2.416**

4 Conclusions

Using the vision technology, the system investigated the LWA-based canopy calculation model and the multi-nozzle application flow calculation model. By studying monocular vision technology to obtain the leaf wall images and the L^* values of the CIELab color space, variable spraying trials were carried out and finally a variable spraying device based on monocular vision was successfully developed. The main results of this study are as follow:

1) The use of image processing techniques for spray volume decision making, including the improvement of the original ExG, makes the reference values obtained for the canopy parameters more true with an error of only 0.5%, indicating that the proposed monocular camera-based acquisition of canopy information has good accuracy; combined with the L^* value of the CIELab color space as the decision coefficient for the variable spray and the L^* value as the reference value for the canopy sparsity, it is verified in the study that there is a relationship between the two. In spite of this, the paper does not discuss the relationship between the two further, the aim is to next plan to explore the more specific relationship that exists between the two.

2) In order to achieve accurate variable spraying, the application volume calculation model under multiple nozzles was developed and analyzed. The spray characteristics of a multi-nozzle variable spraying system are not a simple superposition of individual nozzles, but a four-nozzle flow model in this system with an effective maximum duty cycle of 65% and a minimum duty cycle of 15%. Although the decision coefficient for the spray flow model was 94%, it still fell short of the ideal value during the system performance validation tests and could be further improved for this purpose.

3) The results of the field tests showed that the prototype with the variable spraying system had the effect of refining the droplet size while keeping the droplet cover-age basically unchanged, with $D_{V0.1}$, $D_{V0.5}$ and $D_{V0.9}$ reducing by 2 μm, 5 μm and 18 μm, respectively. The droplet coverage density was increased by 27 droplets/cm^2; better droplet distribution uniformity and droplet penetration were obtained under the effect of water hammer, with a 16% increase in droplet distribution uniformity and a 3% increase in droplet penetration, and a saving of approximately 55.64% in the amount of pesticide used, indicating that the spray prototype could improve spray performance to some extent.

Acknowledgements

This research was financially supported by Guangzhou Science and Technology Plan Project (Grant No. 202002030245). It was also partly supported by the National Natural Science Foundation of China (Grant No. 31671591 and 31971797), Guangdong Province Modern Agricultural Key Technology Model Integration and Demonstration and Promotion Project (2021), Guangdong Province Modern Agricultural Industry Technology System Innovation Team Construction Special Fund (Grant No. 2021KJ108); Guangdong Provincial Education Department Special Innovation Category Project (Grant No. 2019KTSCX013); Guangdong Provincial Science and Technology Innovation Strategy Special Funds in 2020 ("Climbing Plan" Special Funds, Grant No. pdjh2020a0084); Guangdong Provincial Students' Innovation and Entrepreneurship Project in 2020 (Grant No. S202010564150).

[References]

[1] Popusoi D. China's policy on agroecology-How Chinese farmers interact with policies and regulations. Central China Normal University, 2018; 99p.

[2] Sun D Z, Zhan X R, Liu W K, Xue X Y, Xie J X, Li Z, et al. Compensation of spray angle to droplet drift under crosswind. Transactions of the CSAE, 2021; 37(21): 80–89. (in Chinese)

[3] Schebesta H, Candel J J. Game-changing potential of the EU's Farm to Fork Strategy. Nature Food, 2020; 1(10): 586–588.

[4] Giles D K, Comino J A. Variable flow control for pressure atomization nozzles. SAE Technical Paper Series, No. 891836. 1989; pp.237–249.

[5] Grella M, Gioelli F, Marucco P, Zwertvaegher I, Mozzanini E, Mylonas N, et al. Field assessment of a pulse width modulation (PWM) spray system applying different spray volumes: duty cycle and forward speed effects on vines spray coverage. Precision Agric, 2022; 23(1): 219–252.

[6] Chen L M, Wallhead M, Zhu H P, Fulcher A. Control of insects and diseases with intelligent variable-rate sprayers in ornamental nurseries. Journal of Environmental Horticulture, 2019; 37(3): 90–100.

[7] Salcedo R, Zhu H P, Zhang Z H, Wei Z, Chen L M, Ozkan E, et al. Foliar deposition and coverage on young apple trees with PWM-controlled spray systems. Computers and Electronics in Agriculture, 2020; 178: 105794. doi: 10.1016/j.compag.2020.105794.

[8] He X K. Research progress and developmental recommendations on precision spraying technology and equipment in China. Smart Agriculture, 2020; 2(1): 133–146. (in Chinese)

[9] Campos J, Gallart M, Llop J, Ortega P, Salcedo R, Gil E. On-farm evaluation of prescription map-based variable rate application of pesticides in vineyards. Agronomy, 2020; 10(1): 102. doi: 10.20944/PREPRINTS201911.0306.V1.

[10] Miranda-Fuentes A, Rodríguez-Lizana A, Gil E, Agüera-Vega J, Gil-Ribes J A. Influence of liquid-volume and airflow rates on spray application quality and homogeneity in super-intensive olive tree canopies. Science of the Total Environment, 2015; 537: 250–259.

[11] Jiang S J, Ma H T, Yang S H, Zhang C, Su D, Zheng Y J, et al. Target detection and tracking system for orchard spraying robots. Transactions of the CSAE, 2021; 37(9): 31–39. (in Chinese)

[12] Balsari P, Marucco P, Tamagnone M. A crop identification system (CIS) to optimise pesticide applications in orchards. The Journal of Horticultural Science and Biotechnology, 2009; 84(6): 113–116.

[13] Berk P, Hocevar M, Stajnko D, Belsak A. Development of alternative plant protection product application techniques in orchards, based on measurement sensing systems: A review. Computers and Electronics in Agriculture, 2016; 124: 273–288.

[14] Comba L, Biglia A, Aimonino D R, Barge P, Tortia C, Gay P. 2D and 3D data fusion for crop monitoring in precision agriculture. In: 2019 IEEE International Workshop on Metrology for Agriculture and Forestry (MetroAgriFor). IEEE; 2019; pp.62–67.

[15] Palleja T, Landers A J. Real time canopy density estimation using ultrasonic envelope signals in the orchard and vineyard. Computers and Electronics in Agriculture, 2015; 115: 108–117.

[16] Zhang Z H, Wang X Y, Lai Q H, Zhang Z G. Review of variable-rate sprayer applications based on real-time sensor technologies. in Automation in Agriculture – Securing Food Supplies for Future Generations. Intech, 2018; pp.53–79. doi: 10.5772/intechopen.73622.

[17] Zhao D J, Zhang B, Wang X L, Guo H H, Xu S B. Automatic Target of Indoor Spray Robot Based on Image Moments. Transactions of the CSAM, 2016; 47(12): 22–29. (in Chinese)

[18] Yan C G, Xu L M, Yuan Q C, Ma S, Niu C, Zhao S J. Design and experiments of vineyard variable spraying control system based on binocular vision. Transactions of the CSAE, 2021; 37(11): 13–22. (in Chinese)

[19] Milella A, Marani R, Petitti A, Reina G. In-field high throughput grapevine phenotyping with a consumer-grade depth camera. Computers and Electronics in Agriculture, 2019; 156: 293–306.

[20] Walklate P J, Cross J V. An examination of Leaf-Wall-Area dose expression. Crop Protection, 2012; 35: 132–134.

[21] Xue X Y, Xu X F, Li Z, Hong T S, Xie J X, Chen J Z, et al. Design and test of variable spray model based on leaf wall area in orchards. Transactions of the CSAE, 2020; 36(2): 16–22. (in Chinese)

[22] Gonnet J F. Colour effects of co-pigmentation of anthocyanins revisited—1. A colorimetric definition using the CIELAB scale. Food Chemistry, 1998; 63(3): 409–415.

[23] Revantino, Mangkuto R A, Suprijanto, Soelami F X N. The impact of correlated colour temperature variation from a tuneable LED lamp on colour sample appearance shift in CIELAB colour space. International Journal for Light & Electron Optics, 2022; 267: 169707. doi: 10.1016/j.ijleo.2022. 169707.

[24] Wang H, Chen X Y, Zhang J X. Characteristic analysis of young red wine from the eastern foot of Helan Mountain based on CIELab color space parameters. Food Science, 2014; 35(9): 20–23. (in Chinese)

[25] Wang L, Li H Q, Tian H, Chang F L. Target recognition and variable spraying control system. Journal of Chinese Agricultural Mechanization, 2016; 37(9): 75–77, 87. (in Chinese)

[26] Woebbecke D M, Meyer G E, Von Bargen K, Mortensen D A. Color indices for weed identification under various soil, residue, and lighting

conditions. Transactions of the ASAE, 1995; 38(1): 259–269.
[27] Jiang H H, Liu L M, Liu P Z, Wang J Y, Zhang X H, Gao D S. Online Calculation Method of Fruit Trees Canopy Volume for Precision Spray. Transactions of the CSAM, 2019; 50(7): 120–129. (in Chinese)
[28] Li L L, He X K, Song J L, Wang X N, Jia X M, Liu C H. Design and experiment of automatic profiling orchard sprayer based on variable air volume and flow rate. Transactions of the CSAE, 2017; 33(1): 70–76. (in Chinese)
[29] Liu Z Z, Xu H H, Hong T S, Zhang W Z, Zhu Y Q, Zhang K. Key Technology of Variable-rate Spraying System of Online Mixing Pesticide. Transactions of the CSAM, 2009; 40(12): 93–96, 129. (in Chinese)
[30] Wei X H, Jiang B, Sun H W, Xu L Q. Design and Test of Variable Rate Application Controller of Intermittent Spray Based on PWM. Transactions of the CSAM, 2012; 43(12): 87–93, 129. (in Chinese)
[31] Zhai C Y. Research on orchard target on-line probing method and air-blast variable spraying technology. Northwest A&F University, 2012; 133p.
[32] Butts T R, Butts L E, Luck J D, Fritz B K, Hoffmann W C, Kruger G R. Droplet size and nozzle tip pressure from a pulse-width modulation sprayer. Biosystems Engineering, 2019; 178: 52–69.
[33] Liu Z M, Wang D X, Wang D G. Handbook of Hydraulic Structure Design. Beijing: China Water & Power Press, 2011; 844p.
[34] Wang C L, Song J L, He X K, Wang Z C, Wang S L, Meng Y H. Effect of flight parameters on distribution characteristics of pesticide spraying droplets deposition of plant-protection unmanned aerial vehicle. Transactions of the CSAE, 2017; 33(23): 109–116. (in Chinese)
[35] Maghsoudi H, Minaei S, Ghobadian B, Masoudi H. Ultrasonic sensing of pistachio canopy for low-volume precision spraying. Computers and Electronics in Agriculture, 2015; 112: 149–160.
[36] Pérez-Ruiz M, Agüera J, Gil J A, Slaughter DC. Optimization of agrochemical application in olive groves based on positioning sensor. Precision Agric, 2011; 12(4): 564–575.
[37] Fan D Q, Zhang M N, Pan J, Lyu X L. Development and Performance Test of Variable Spray Control System Based on Target Leaf Area Density Parameter. Smart Agriculture, 2021; 3(3): 60–69. (in Chinese)